14:45:01 OCA PAD INITIATION - PROJECT HEADER INFORMATION 06/20/90

Active

Project #: E-25-M45 Cost share #: Rev #: 0
Center # : 10/24-6-R6969-0A0 Center shr #: OCA file #:
Work type : RES
Contract#: N00014-90-J-1944 Mod #: Document : GRANT
Prime #: Contract entity: GTRC

Subprojects ? : N
Main project #:

Project unit: ME Unit code: 02.010.126
Project director(s):
BAIR S S III ME (404)894-3273
WINER W O ME (404)-

Sponsor/division names: NAVY / OFC OF NAVAL RESEARCH
Sponsor/division codes: 103 / 025

Award period: 900601 to 910131 (performance) 910131 (reports)

Sponsor amount	New this change	Total to date
Contract value	52,908.00	52,908.00
Funded	52,908.00	52,908.00
Cost sharing amount		0.00

Does subcontracting plan apply ?: N

Title: DEFORMATION BEHAVIOR OF THIN LUBRICANT FILMS AT ELEVATED PRESSURE

PROJECT ADMINISTRATION DATA

OCA contact: E. Faith Gleason 894-4820

Sponsor technical contact

PETER P. SCHMIDT
(202)696-4325

OFFICE OF THE CHIEF OF NAVAL
RESEARCH, CODE 1131N
800 NORTH QUINCY STREET
ARLINGTON, VA 22217-5000

Sponsor issuing office

EVELYON FIELDS
(202)696-4508

OFFICE OF NAVAL RESEARCH
CODE 1513/ETF
800 NORTH QUINCY STREET
ARLINGTON, VA 22217-5000

Security class (U,C,S,TS) : U ONR resident rep. is ACO (Y/N): Y
Defense priority rating : N/A ONR supplemental sheet
Equipment title vests with: Sponsor GIT X

Administrative comments -
* INITIATION.

GEORGIA INSTITUTE OF TECHNOLOGY
OFFICE OF CONTRACT ADMINISTRATION

NOTICE OF PROJECT CLOSEOUT

SR852

Closeout Notice Date 04/22/93

Project No. E-25-M45 Center No. 10/24-6-R6969-0A0

Project Director BAIR S S III School/Lab MECH ENGR

Sponsor NAVY/OFC OF NAVAL RESEARCH

Contract/Grant No. N00014-90-J-1944 Contract Entity GTRC

Prime Contract No.

Title DEFORMATION BEHAVIOR OF THIN LUBRICANT FILMS AT ELEVATED PRESSURE

Effective Completion Date 910131 (Performance) 910131 (Reports)

Closeout Actions Required:	Y/N	Date Submitted
Final Invoice or Copy of Final Invoice	Y	
Final Report of Inventions and/or Subcontracts	Y	
Government Property Inventory & Related Certificate	Y	
Classified Material Certificate	N	
Release and Assignment	Y	
Other	N	

Comments EFFECTIVE DATE 6-1-90. CONTRACT VALUE $52,908.

Subproject Under Main Project No.

Continues Project No.

Distribution Required:

Project Director	Y
Administrative Network Representative	Y
GTRI Accounting/Grants and Contracts	Y
Procurement/Supply Services	Y
Research Property Managment	Y
Research Security Services	N
Reports Coordinator (OCA)	Y
GTRC	Y
Project File	Y
Other HARRY VANN-FMD	Y
FRED CAIN-OOD	Y

NOTE: Final Patent Questionnaire sent to PDPI.

DEFORMATION BEHAVIOR OF THIN LUBRICANT FILMS AT ELEVATED PRESSURE

July, 1991

A Report to the

Office of Naval Research
800 North Quincy Street
Arlington, VA 2217-5000

by

Scott Bair
Senior Research Engineer

F. Qureshi
Graduate Research Assistant

W. O. Winer
Regents' Professor and Director

George W. Woodruff School of Mechanical Engineering
Georgia Institute of Technology

SUMMARY

Results to date with the Flow Visualization Cell confirm the existence of inhomogeneous deformation in liquid lubricants at high pressure in the form of shear bands.

A High Pressure Flow Visualization Cell has been designed and constructed to perform a fundamental investigation of the deformation behavior of liquid lubricants under lubricated concentrated contact conditions. A pressure of 0.3 GPa and a shear stress in Couette shear of about 25 MPa has been demonstrated. Time averaged velocity profiles show no discontinuities (slip) either in the bulk or at walls. Localized slip at shear bands inclined to the walls was demonstrated to occur during non-linear shear response. The number of shear bands increases with shear rate (and shear stress) from as few as one at the onset of non-Newtonian flow until the shear region is essentially filled with bands with a spacial periodicity of 7 μm. Bands are typically inclined 19° off the solid surfaces in a direction which reduces the compressive normal stress due to shear on the plane of the band.

1. INTRODUCTION

The origin of traction in the elastohydrodynamic (EHD) lubrication of concentrated contacts has been a vexing problem that has plagued researchers for years. Linear Newtonian behavior fails spectacularly in predicting EHD frictional traction. The fact that traction in EHD seldom exceeds one-tenth of the average pressure and that this could not be explained in terms of a Newtonian viscous fluid led Smith (1959) to propose a limiting shear stress for the lubricant. That is, that the lubricant flows as a plastic solid at some shear stress which varies with temperature and pressure. This concept has been supported by numerous primary high-pressure measurements (Bair and Winer, 1979 and 1990, and Ramesh and Clifton, 1987).

The transition from linear Newtonian behavior to rate-independent (plastic) behavior is illustrated by the steady shear flow curves in Figure 1. Here, the logarithm of shear stress is plotted versus logarithm of shear rate for a polyphenol ether (5P4E) and a mineral oil (N1). Shear stress is observed to increase first in proportion to shear rate (Newtonian) - then a non-linear transition region occurs - followed by continuous shearing at a limiting stress, τ_L. This limiting stress is approximately proportional to pressure. Elastic effects are observed for transient loading in shear (Bair and Winer, 1979). The recoverable elastic strain is typically 0.02 to 0.03. Because the glass transition temperature increases with pressure,

many liquid lubricants are below the glass transition temperature in concentrated contact (Alsaad, et.al., 1978). In Figure 1, $\tilde{p}^{*}$ is the ratio of pressure to glass transition pressure.

As of this time the limiting shear stress concept lacks a firm theoretical foundation. Evans and Johnson (1986) proposed a mechanism by which the non-linear transition is attributed to the thermal activation model of Eyring and the rate-independent behavior is explained by shear bands as occur in the deformation of solid polymers. Bair and Winer (1990) showed that the dislocation model of Gilman (1975) for amorphous metals predicts the pressure dependence of the limiting stress. Many have suggested wall slip and Kaneta et.al. (1990) have presented an inconclusive argument based on EHD film thickness observations to support wall slip. All of these mechanisms incorporate some type of shear localization.

It is the objective of this program to perform a fundamental investigation of the shear deformation of liquid lubricant films at high-pressure to elucidate the flow mechanisms which produce the observed rheological behavior. Toward this end, flow visualization experiments have been designed and conducted.

2. EXPERIMENTAL

2.1 Technique

In order to visualize the shear deformation of liquid lubricant films at elevated pressure, a test cell must shear a liquid sample in such a manner that the sample may be illuminated and local displacements or velocities be viewed and measured. To simplify interpretation of results, the Couette shear configuration was selected. A schematic drawing of the flow visualization configuration is given in Figure 2. The liquid sample is sheared between the end of a stationary shaft (pin) and a flat on the side of a moving shaft. The moving shaft translates axially. Illumination and viewing are at right-angles to the axes of both shafts.

Two techniques for flow velocity measurement were considered: laser doppler velocimetry and particle tracing. The former technique was rejected due to the rather large (compared to the film thickness) spatial resolution. However, the present flow cell may be adaptable to other measurement techniques not yet considered.

Originally, carbon black with 0.3 μm particle size was used as a tracer because of its opacity. This material agglomerates into larger particles of various sizes. It was quickly found that the larger of these particles could be seen far from the plane of focus of the microscope. Since it is imperative that only particles within the shearing gap be seen and preferable that only particles near the focal plane be visible, the smallest visible particle should be selected. Commercially

available polystyrene tracer spheres with fluorescent dye were found to be soluable in lubricants. Glass spheres of 2 μm diameter were found to be visible in one of our model lubricants (5P4E)-apparently due to the difference in retractive index. These particles are not visible at more than 0.1mm from the focal plane.

2.2 Test Cell

A proof-of-concept prototype of the Flow Visualization Cell was constructed so that the technique might be proven at atmospheric pressure before embarking on the design of a high-pressure version. It was determined that the motion of carbon black particles could be tracked in a 100 μm thick film in Couette shear using a reflecting objective microscope with long (24mm) working distance.

The final design of the High-Pressure Flow Visualization Cell is shown in Figure 3 in cut-away. The internal components are symmetric about the cutting plane through the stationary shaft so that the entire cell interior need not be shown. The stationary shaft or pin is hollow to accept a thermocouple and is clamped to the pressure vessel. The moving shaft extends completely through the vessel to balance the hydrostatic force upon it. The shearing gap may be varied from 0 to 200 μm by rotating the moving shaft although the boundaries are only exactly parallel for one gap dimension. Illumination is usually through the lower window.

A beam splitting prism in the optics allows illumination from above for finding the top of the gap.

The moving shaft passes through one isolating piston and one high-pressure seal at each end. The pressurizing medium , a diester, is admitted between the high-pressure seal and the isolating piston through a port in the back of the cell. The moving shaft is driven axially by a hydraulic cylinder (not shown in the figure) and positioned rotationally by a worm and gear (also not shown). The axial displacement of this shaft is measured by an LVDT external to the cell.

Windows are sapphire and are sealed to the closures by a lapped fit. Temperature of the cell is controlled by either a resistance heater or liquid nitrogen boil-off passing through an aluminum block which is fastened to the exterior of the cell. Temperature is measured at the thermocouple in the hollow stationary shaft (pin).

Initially, the moving shaft was driven hydraulically by kerosene from a variable displacement metering pump. It was soon found that the vibration of the pump motor caused the small (2μm) tracer particles to disappear from view. Bottled gas was used thereafter in place of the pump.

The cell was pressure tested at 350 MPa and results have been obtained at 270 MPa.

2.3 Optics

A prerequisite for a microscope objective used to view material within a pressure cell is a long working distance to accomodate the thick pressure vessel walls. In this case, the minimum working distance is about 20 mm - longer if filters are placed between the cell and objective. Also a high magnification is required in order to keep the gap and tracer particles small. For these reasons, a reflecting objective (15X) was selected.

Illumination through the lower window is provided by a 150W incandescent variable source through a fibre optic bundle. A 50W incandescent source is provided for illumination from above in order to position the focal plane at the top of the shearing gap as seen in the upper view of Figure 2. A dial indicator mounted to the microscope tube indicates the microscope objective relative working distance so that any position measured into the gap may be selected. However, there is a fundamental problem related to viewing the interior of a cavity with parallel walls in that material near the wall is obscured by the interference of the opaque wall with the acceptance cone of the objective. This effect is such that for each 100μm deeper one moves the focal plane into the gap, 5μm is obscured along the wall. A depth of 200-250μm into the gap was selected for viewing as a compromise between the conflicting requirements of viewing fully-developed flow and seeing material near the walls.

The microscope tube has been adapted to accept video cameras and a 35mm film camera. A high-speed video system of up to 12,000 frames per second was tried. However, insufficient illumination was available for framing rates above 30/sec which is the conventional video rate.

2.4 Experimental Liquid Lubricants

For an exploratory study of lubricant shear rheology, it is advantageous to select as model liquids, materials which have seen application as EHD lubricants and for which much data - both rheological and tribological - are available in the literature. Also, as the velocity measurement technique is limited to low shear rates of less than $10s^{-1}$, it is important that the viscosity be great enough to yield non-Newtonian flow at this shear rate. That is, a shear stress approximately equal to the limiting stress must be obtained at a shear rate of $10s^{-1}$.

The liquids selected are: a mineral oil - LVI 260 and a synthetic oil - 5P4E, a polyphenol ether. These have been characterized extensively in the literature (Johnson and Tevaarwerk, 1977, Bair and Winer, 1982 and 1990, Hutton, 1985, Ramesh and Clifton, 1987).

As a guide in selecting experimental conditions and in interpreting the results, it was necessary to determine the pressure-viscosity characteristics of the experimental liquids. This was done to pressures above the glass transition by a

method outlined by Bair and Winer, 1991. Results are shown in Figure 4 for 5P4E.

It is important to show that the tracer particles have negligible influence on the liquid rheology. This was demonstrated in the Newtonian regime by repeating some of the viscosity measurements with 2μm glass spheres dispersed in the liquid. Weight fractions of 0.1% and 0.5% were employed and are typical of concentrations used in the flow visualization experiments. (Volume fractions are 0.4 of these values.)

The viscosity, μ, was found to be a function of temperature, T, and pressure, p, which could be described by a modified free volume model (Bair and Winer, 1991). The curves in Figure 4 represent

$$\mu = \begin{cases} \mu_g e^{-2.3\left[\frac{C_1\,[T-T_g(p)]\,F(p)}{C_2 + [T-T_g(p)]\,F(p)}\right]}, & p \le p_g \\ \mu_g e^{\alpha_g (P-P_g)}, & p > p_g \end{cases}$$

$$T_g = T_{go} + A_1 \ln(1 + A_2 p)$$

$$F = 1 - B_1 \ln(1 + B_2 p)$$

The glass transition temperature, T_g, is assumed to be an isoviscous state with viscosity, μ_g. Both T_g and the relative free volume expansivity, F vary with pressure. The conventional free volume relation fails above the glass transition

pressure, p_g and is replaced by an exponential relation with a pressure viscosity coefficient, α_g.

3. RESULTS

3.1 Shear Force Measurement

During preliminary measurements it was observed that the stationary shaft or pin deflected a small but measurable distance in the manner of a cantilever beam due to the shear stress at the shearing region and due to the drag of liquid flowing around the pin outside diameter. The relationship between pin deflection and a shear force at the end of the pin (stationary shaft) was calibrated and found to be linear. When the edge of the pin is in view (i.e. the entrance or exit to the shearing region) the shear force can be measured. Unfortunately, the pin deflection is not entirely due to the shear stress in the region of interest. However, if the effective shear force from the drag of the flow around the pin varies linearly with moving shaft speed (and, therefore, with shear rate in the shear region) then, any non-linearity in the steady shear force-shear rate response must be attributed to non-Newtonian flow in the shear region.

This is illustrated by Figure 5 where the pin force is plotted versus shear rate (determined from the moving shaft velocity divided by the gap which was 150μm). A linear proportional behavior is observed up to a force of 100N. If this force is converted to an effective shear stress by dividing the area of the pin end, the non-linearity begins at about 30 MPa. The limiting shear stress at these conditions would be expected to be about 23 MPa from concentric cylinder rheometer measurements (Bair and Winer, 1990). In fact, if the last two measured

points on Figure 5 are assumed to represent rate-independent behavior in the shear region, the force due to free stream drag can be subtracted and a limiting shear stress of 21 MPa results. It must be concluded that a departure from linearity in the pin force/shear rate represents the transition between Newtonian to limiting stress behavior. The viscosity determined in this exercise is 1.7×10^8 Pa s which is in agreement with the viscosity measurements of Figure 4 and is shown as the triangle in that figure.

3.2 Velocity Profiling

Local liquid velocities can be determined from the ratio of particle displacement to the time interval over which the displacement occurred (Muller-Mohnssen, et.al., 1990) assuming that the local particle velocity is identical to the local liquid velocity. Several commercial image analysis systems were utilized in an attempt to automate the particle tracing. All of these systems were found to be incapable of recognizing particles as small as 2μm and as explained previously we prefer not to use larger particles.

Early velocity profiles which indicated slug flow or shear localization at the walls were apparently the result of contamination of the test liquid by the lower viscosity pressurizing medium which had entered the shearing region through the isolating piston.

A typical set of time averaged velocity profiles is shown in Figure 6 for the indicated shear rates. The gap measured 127 μm. The local velocity, u, was found from the displacement of a tracer particle over a time which varied from one to two seconds. The velocity scale is not the same for all plotted profiles. Velocities are corrected for the deflection of the pin and the particle concentration was 0.1% by weight.

A total of about twenty five velocity profiles have been obtained for the liquid 5P4E, for various temperatures, pressures and shear rates. These profiles, which were time averaged over several seconds, indicate a linear velocity variation across the gap. These velocities when extrapolated to the wall position are in good agreement with the wall velocities. (Note that approximately 20 μm of liquid near the wall is obscured.) Then, if wall slip were occurring, it would necessarily be a very small fraction of the relative velocity of the boundary surfaces.

3.3 Shear Bands

It was observed during the velocity profiling that at the higher shear stresses visible artifacts appeared in the form of bands. When polarizing filters were placed between the light source and the cell and/or between the cell and the microscope, thick diffuse colored bands were observed along flow streamlines during stress transients. These are possibly due to birefringence from molecular

alignment in shear. When no optical filters were employed and particularly for low tracer particle concentration very sharp bands were inclined to the liquid boundaries in the manner which has been observed for shear bands in solid polymers (Wu and Li, 1976). It is these sharp inclined shear bands that are of primary interest here and will be examined in more detail in what follows. It will be shown that slip actually occurs along an individual band.

Shear bands are shown in the video prints in Figure 7 along with the shearing direction. These bands appear with an angle of 19° to the solid surfaces and oriented such that they lie in a plane of reduced normal stress due to shear. The inclination angle appears to increase as the band rotates with the continuum a few degrees until the band disappears. The conditions for Figure 7 are 220 MPa, 22°C and a shear rate of $0.25s^{-1}$. The material is 5P4E and the gap is 130μm. When multiple bands form, as in Figure 7, a strong spacial periodicity is seen and the separation is about 7μm measured perpendicular to the band. Shear bands were observed in 5P4E at pressures of 125 to 220 MPa, temperatures of 5 to 22°C and for gaps of 47 to 220μm and in LVI 260 (mineral oil) at a pressure of 270 MPa and 5°C.

The appearance of shear bands is associated with the onset of non-linear shear rheology as shown in Figure 8. The first shear band is observed in the second video print from the left which corresponds to the first data point past the Newtonian regime as described in a previous section. The pressure is 220 MPa

and the temperature is 22°C. This correlation was found at several temperature/pressure combinations. As the pin force (and shear stress) is increased the bands proliferate until they appear to fill the entire shearing region.

The tracer particles which were used to generate velocity profiles can be used to detect slip associated with a band. For this purpose it will be useful to find two particles near the midplane of the shearing region and nearly equidistance from the solid boundaries. The motion of this pair of particles without the influence of a shear band is shown in Figure 9a. Particles A and B move an equal distance in the shear direction over some time interval. If a shear band were operating between these particles, then the motion would be expected to be the same as in Figure 9a except that a slip displacement aligned with the band would be added to the particle motion as shown in Figure 9b. Our ability to measure a particle position is limited to a resolution of about 0.5 μm. Therefore, it is convenient to place a coordinate system, XY, on particle A as in Figure 9c. (Recall that these particles are equidistance from the boundaries.) Now, if there is no slip the X and Y coordinates of B will not change over a time interval during which a band exists between A and B. If slip occurs, the total slip will be the change in X and Y during that time interval, ΔX and ΔY respectively. Video tapes were reviewed to find pairs of particles which satisfied the above geometric requirements and for which a single shear band passed between. The displacement of B with respect to A is plotted for one such pair in Figure 10. The

displacement at the indicated time is relative to time zero. Straight lines were drawn between readings which were taken at 1, 2, and 3 seconds although the actual history between readings is not known, A shear band was visible for some time between 1 and 2 seconds and not for the previous and succeeding interval. The relative displacements were consistent with slip along the band.

The total slip, $\sqrt{\Delta X^2 + \Delta Y^2}$ is tabulated along with the slip direction, $\tan^{-1} \Delta Y/\Delta X$ for three examples. The first entry in the Table is that of Figure 10. Recalling that our resolution is 0.5 μm, the slip direction is consistent with the observed band orientation.

4.0 CONCLUSION

A High Pressure Flow Visualization Cell has been designed and constructed to perform a fundamental investigation of the deformation behavior of liquid lubricants under lubricated concentrated contact conditions. A pressure of 0.3 GPa and a shear stress in Couette shear of about 25 MPa has been demonstrated. Time averaged velocity profiles show no discontinuities (slip) either in the bulk or at walls. Localized slip at shear bands inclined to the walls was demonstrated to occur during non-linear shear response. The number of shear bands increases with shear rate (and shear stress) from as few as one at the onset of non-Newtonian flow until the shear region is essentially filled with bands with a spacial periodicity of 7μm. Bands are typically angled 19° off of the solid surfaces in a direction which reduces the compressive normal stress due to shear on the plane of the band. Of course, continuity requires that slip not extend to the boundary. The shear band may turn tangent to the wall or end near the boundary. According to Haward (1973) shear bands may be wholly contained within the body accommodated by elastic deformation between the ends of the bands and the boundaries.

5.0 RECOMMENDATIONS

Results to date with the Flow Visualization Cell confirm the existence of inhomogeneous deformation in liquid lubricants at high pressure in the form of shear bands. Future work should extend measurements to additional lubricant chemical structures. Additional work must be done to elucidate the slip criterion which controls shear band formation. Theoretical modeling should be performed to permit generalization of the concept. For this purpose measurements should be made of:

1) Shear band slip as a function of distance from walls.

2) Shear band angle as a function of pressure and chemical structure.

3) Shear band operating time as a function of shear rate.

Also, modifications should be made to the cell to raise the shear stress capability and reduce the minimum gap to more closely simulate lubricated contacts.

TABLE. RELATIVE DISPLACEMENTS OF PARTICLES ASTRIDE SHEAR BANDS

5P4E

PRESSURE MPa	TEMP. °C	SHEAR RATE s^{-1}	$\sqrt{\Delta X^2 + \Delta Y^2}$ μm	$\tan^{-1} \Delta Y/\Delta X$
130	5	0.12	3.9	19°
130	5	0.13	5.0	20°
130	5	0.34	5.9	29°

REFERENCES

Alsaad, M., Bair, S., Sanborn, D. M., and Winer, W. O., (1978), "Glass Transitions in Lubricants: Its Relation to EHD Lubrication," **Trans. ASME, Journal of Lubrication Technology**, 100, 2, p. 404-417.

Bair, S. and Winer, W. O., (1979a), "Shear Strength Measurements at High Pressure," **Trans. ASME, Journal of Lubrication Technology**, 101, 3.

Bair S. and Winer, W. O., (1979b), "A Rheological Model for Elastohydrodynamic Contacts Based on Primary Laboratory Data," **Trans. ASME, Journal of Lubrication Technology**, 101, 3, p. 258-265.

Bair, S. and Winer, W. O., (1982), "Some Observations in High Pressure Rheology of Lubricants," **Trans. ASME, Journal of Lubrication Technology**, 104, 3, p. 382-386.

Bair S. and Winer, W. O., (1990), "The High Shear Stress Rheology of Liquid Lubricants at Pressures of 2 to 200 MPa", **Trans. ASME, Journal of Tribology,** 112, No. 2.

Bair, S. and Winer, W. O., (1991) "The High Pressure High Shear Stress Rheology of Liquid Lubricants", **Trans. ASME, Journal of Tribology**, Accepted for Publication.

Evans, C. R. and Johnson, K. L., (1986), "The Rheological Properties of EHD Lubricants," **Proc. Instn. Mech. Engrs.**, Vol. 200, No. C5.

Gilman, John J., (1975), "Mechanical Behavior of Metallic Glasses", **Journal of Applied Physics**, Vol. 46, No. 4.

Haward, R. N., (1973), **The Physics of Glassy Polymers**, John Wiley & Sons.

Hutton, J. F., (1985), "Re-assessment of Rheological Properties of LVI 260," **Trans. ASME, JOLT**, 106, p. 537.

Muller-Mohnssen, Weiss, D., and Trippe, A., (1990) "Concentration Dependent Changes of Apparent Slip in Polymer Solution Flow", **Journal of Rheology**, 34, (2), p. 227.

Johnson K. L. and Tevaarwerk, J. L., (1977), "Shear Behavior of Elastohydrodynamic Oil Films," **Proc. Roy. Soc. of London**, 365A, pp. 215-236.

Kaneta, M., Nishikawa, H., and Kameishi, K., (1990), "Observation of Wall Slip in Elastohydrodynamic Lubrication", **Journal of Tribology, ASME**, Vol. 112, p. 447.

Ramesh, K. T. and Clifton, R. J., (1987), "A Pressure Shear Plate Experiment for Studying the Rheology of Lubricants at High Pressures and High Shearing Rates," **Trans. ASME, Journal of Tribology**, Vol. 109, No. 2.

Smith, F. W., (1959), "Lubricant Behavior in Concentrated Contact Systems - The Caster Oil-Steel System," **Wear,** Vol. 2, No. 4, p. 260-263.

Wu, J. B. C. and Li, J. C. M., (1976), "Slip Processes in the Deformation of Polystyrene", **Journal of Materials Sci. 11**, p. 434-444.

Yasutomi, S., Bair, S., and Winer, W. O., (1984), "An Application of a Free Volume Model to Lubricant Rheology," **Trans. ASME, Journal of Tribology**, 106, 2.

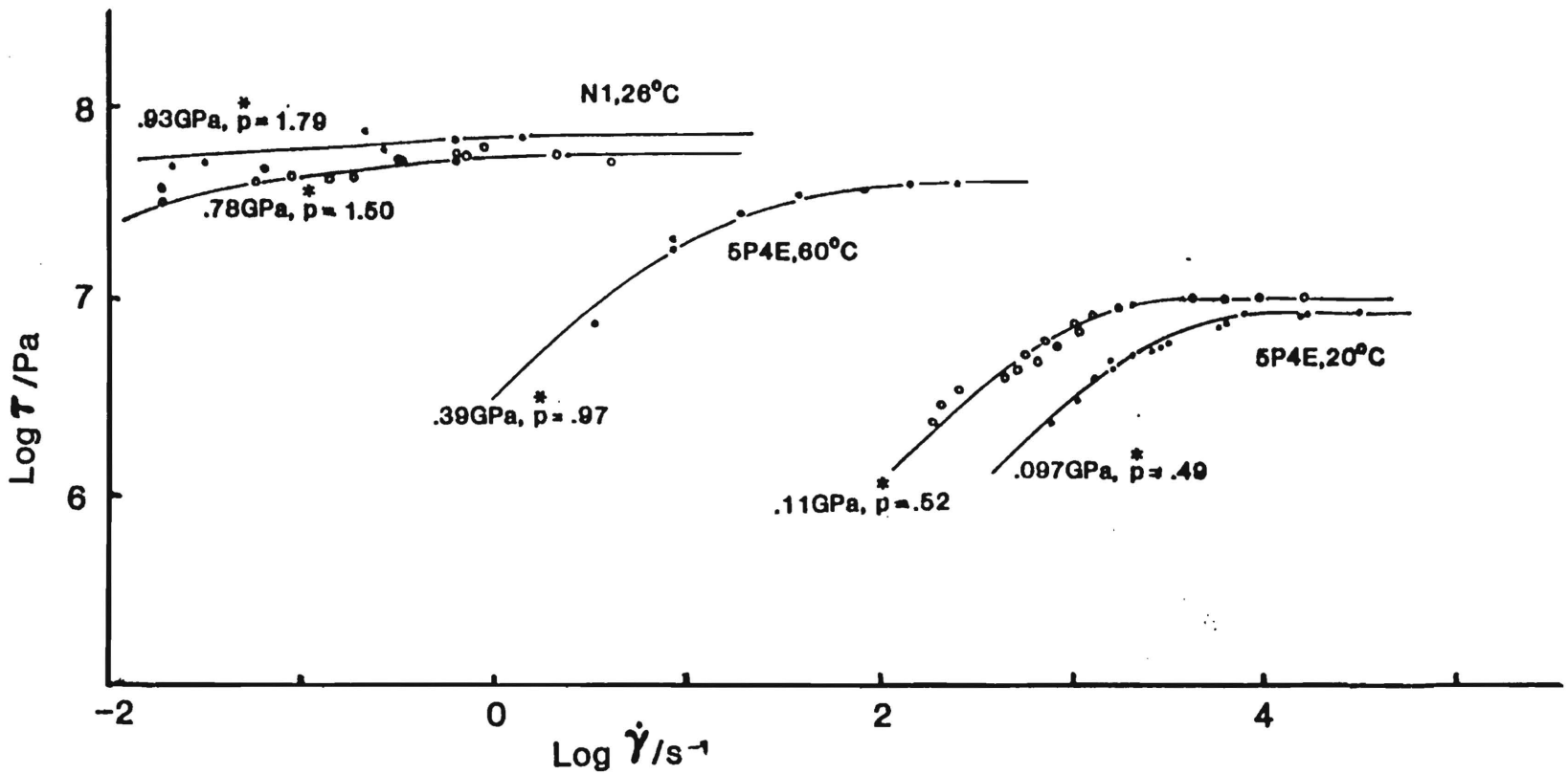

Figure 1. The Transition From Newtonian to Plastic Flow for Various Dimensionless Pressures. τ is Shear Stress and $\dot{\gamma}$ Shear Rate.

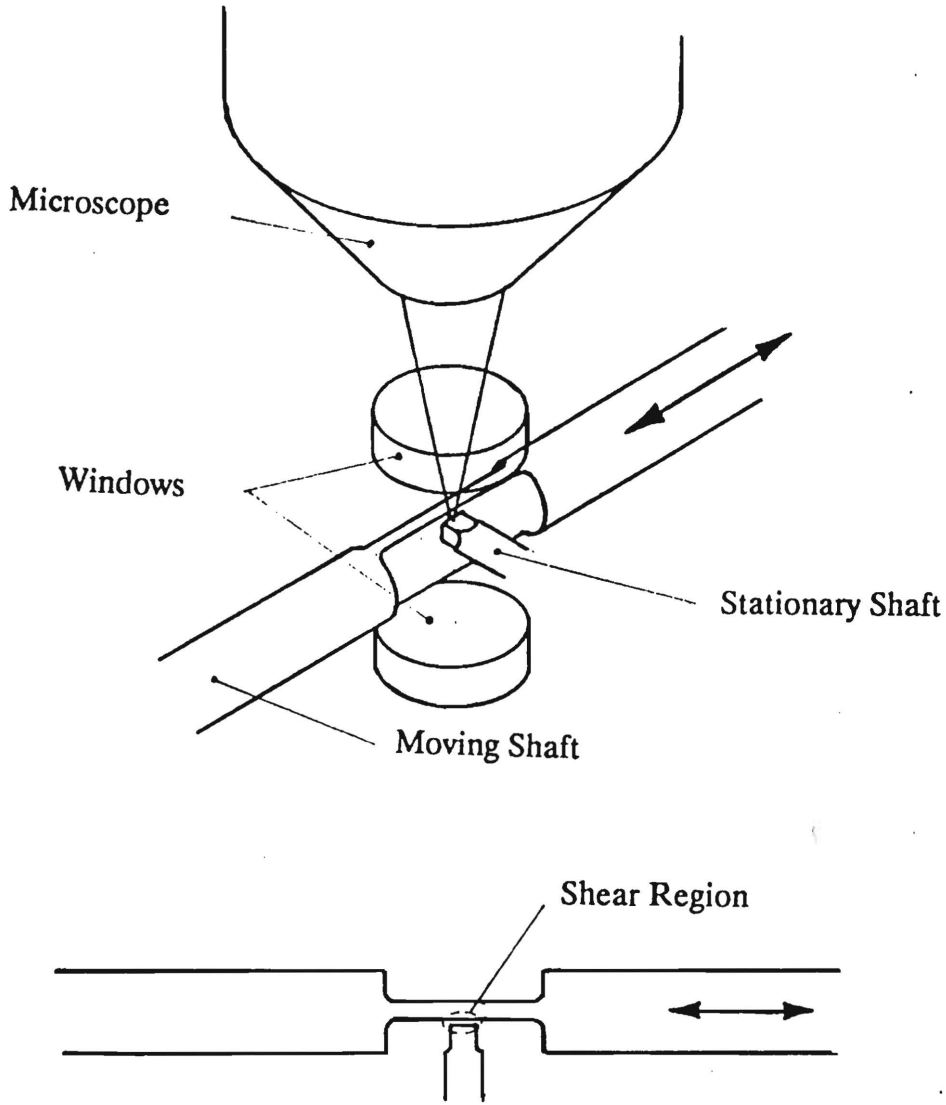

Figure 2. Flow Visualization Configuration. (Illumination Through Lower Window.)

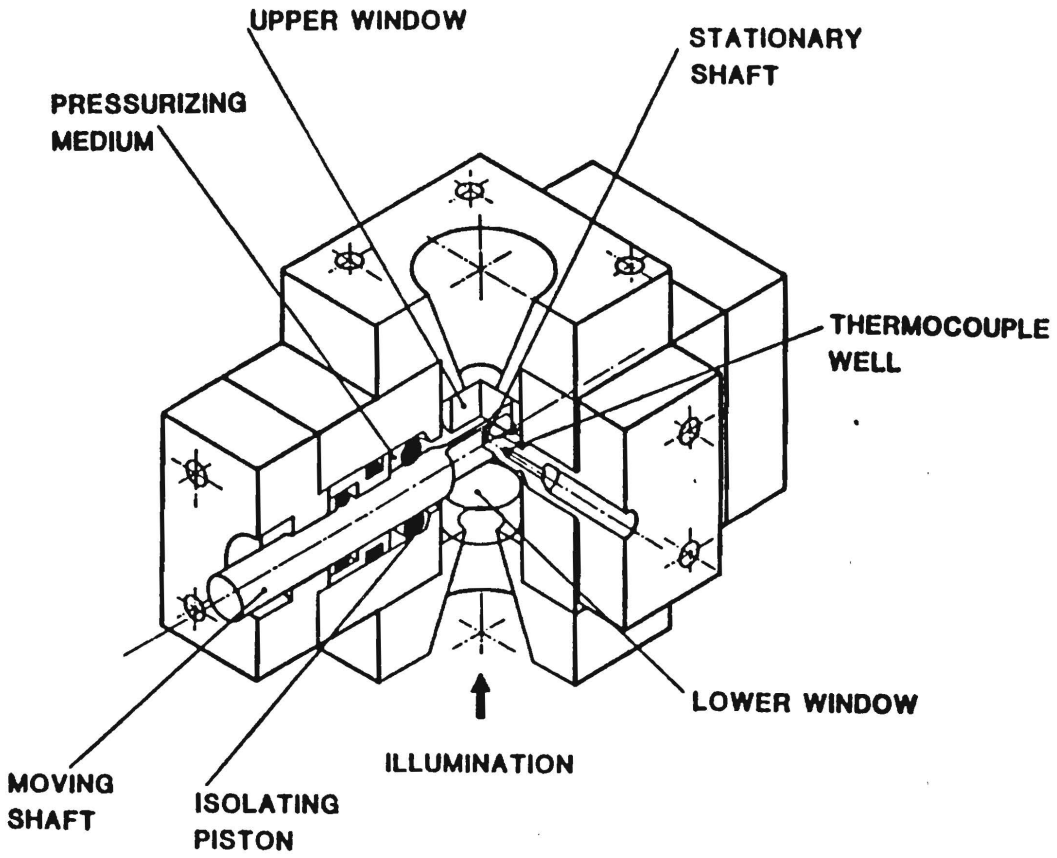

Figure 3. High-Pressure Flow Visualization Cell.

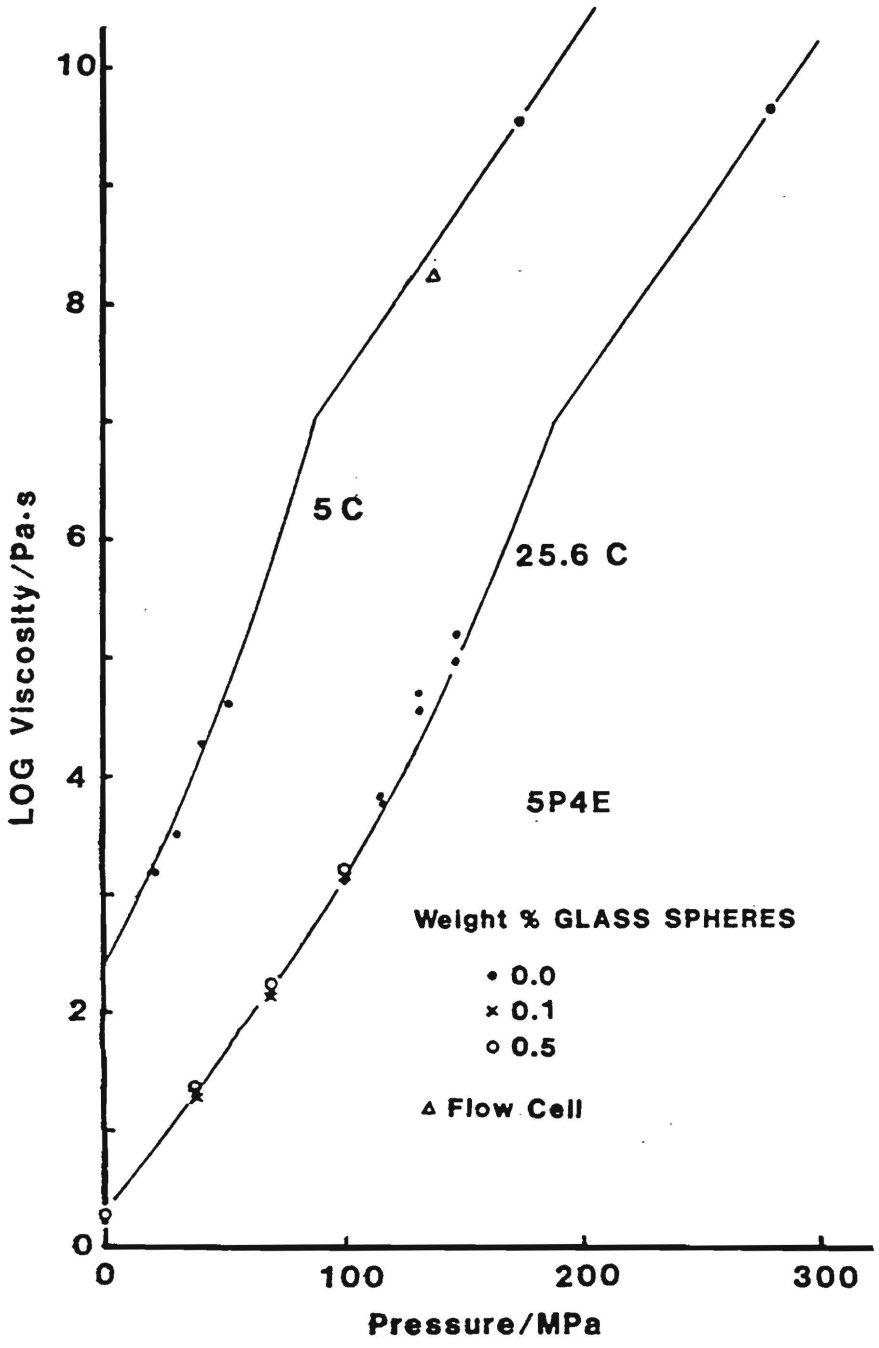

Figure 4. Pressure-Viscosity of *5P4E* and the Effect of the 2μm Tracer Particles.

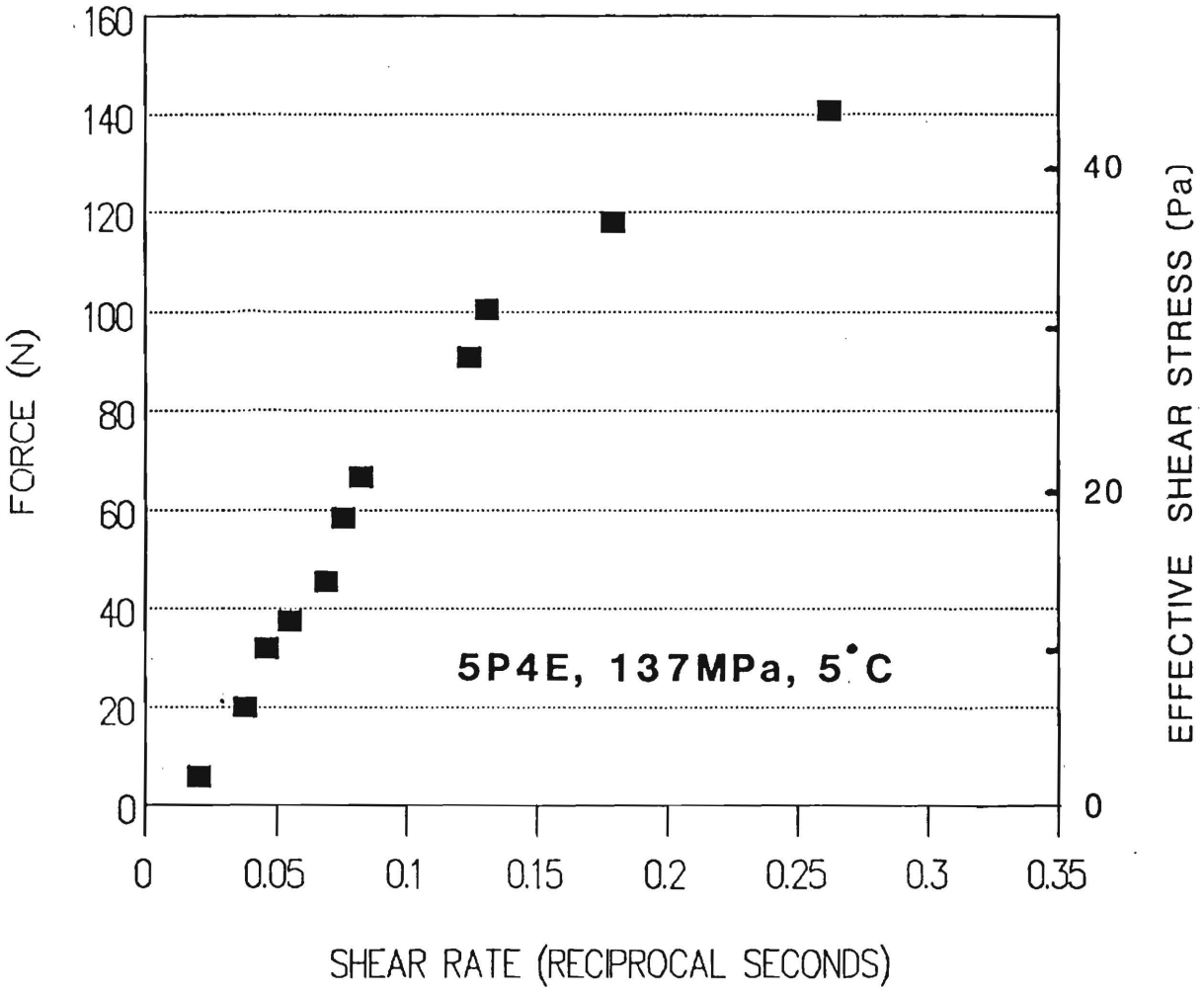

Figure 5. Pin Force Versus Overall Shear Rate.

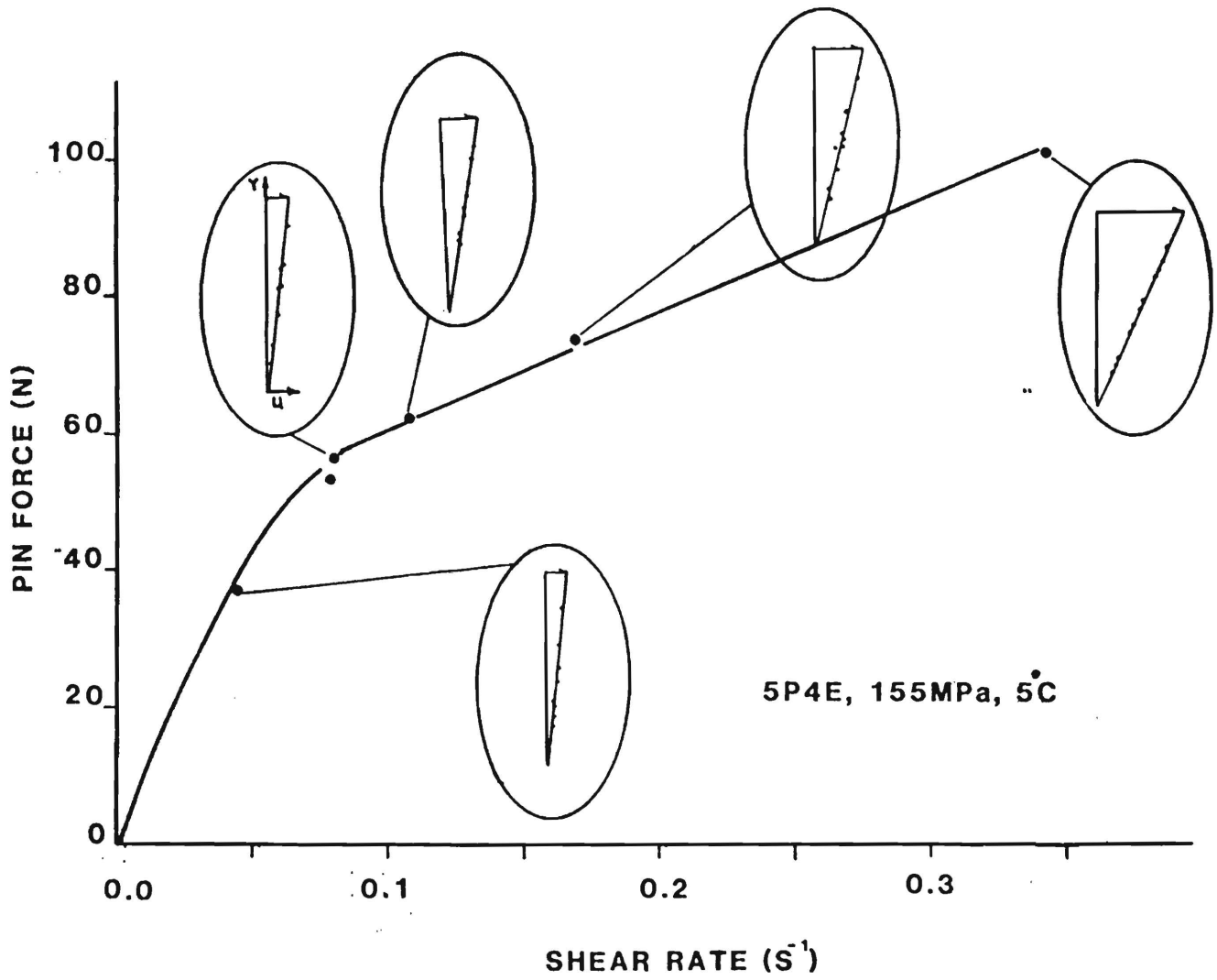

Figure 6. Velocity Profiles.

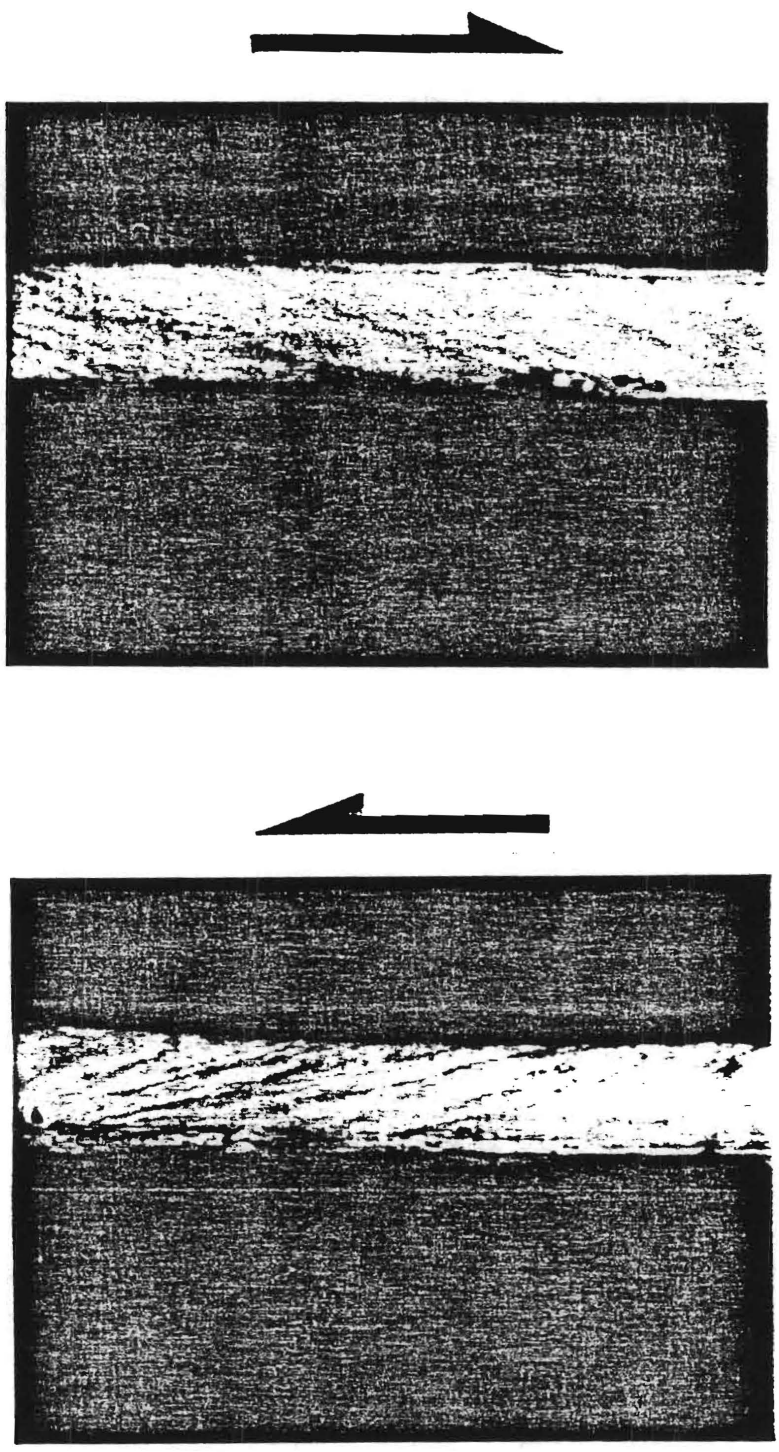

Figure 7. Shear Bands in 5P4E at 220 MPa, 22°C, and Shear Rate of 0.25 s^{-1}.

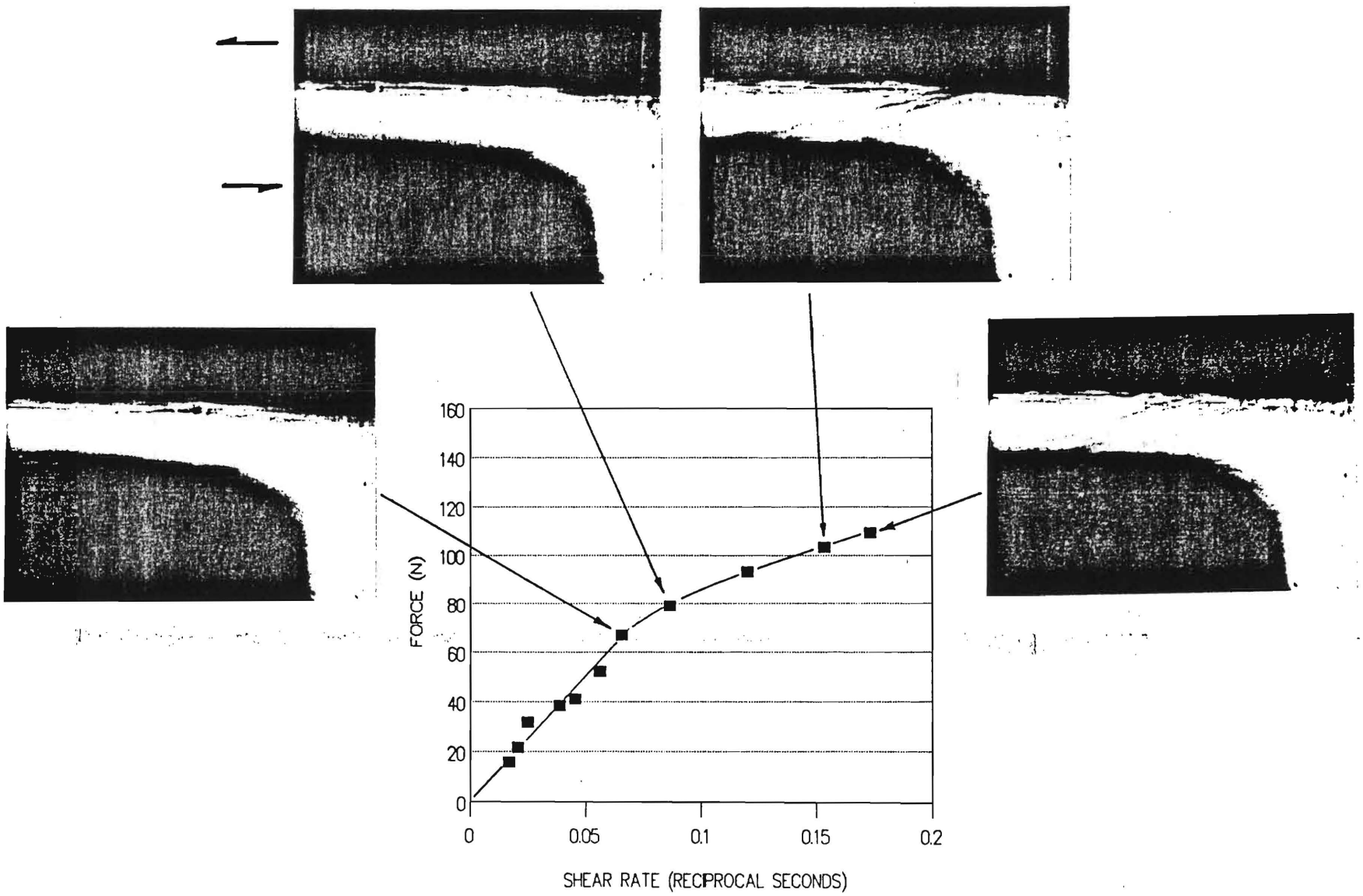

Figure 8. Shear Bands Are Associated With Non-Linear Behavior.

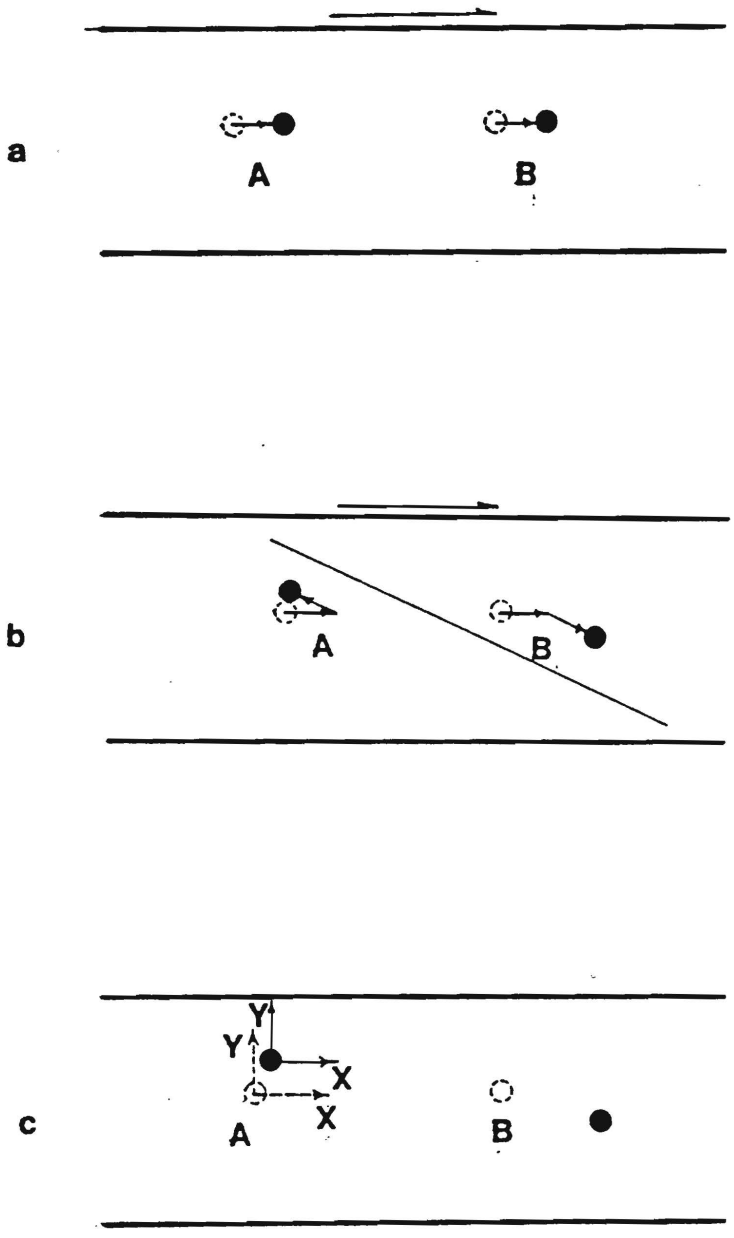

Figure 9. Particle Motion Under Influence of a Shear Band.

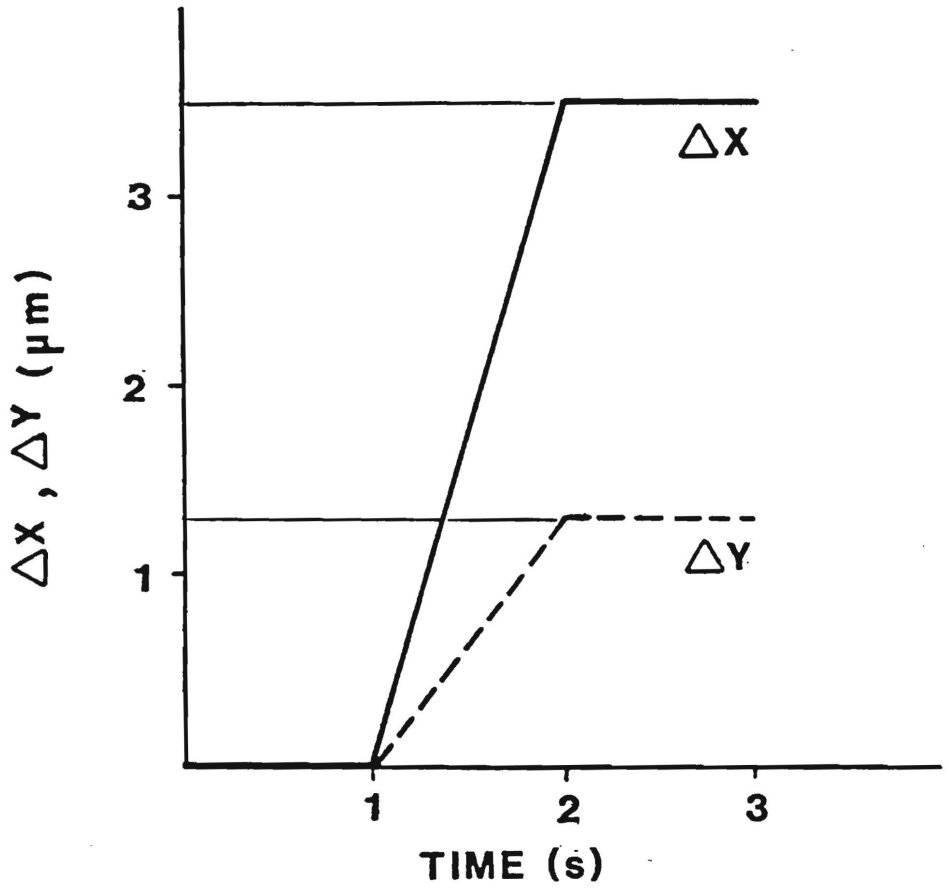

Figure 10. Relative Displacement of a Pair of Particles Astride a Shear Band.